EURASIP Journal on Advances in Signal Processing
a SpringerOpen Journal

RESEARCH Open Access

Fault detection for hydraulic pump based on chaotic parallel RBF network

Chen Lu[1,2*], Ning Ma[2,3] and Zhipeng Wang[1,2]

Abstract

In this article, a parallel radial basis function network in conjunction with chaos theory (CPRBF network) is presented, and applied to practical fault detection for hydraulic pump, which is a critical component in aircraft. The CPRBF network consists of a number of radial basis function (RBF) subnets connected in parallel. The number of input nodes for each RBF subnet is determined by different embedding dimension based on chaotic phase-space reconstruction. The output of CPRBF is a weighted sum of all RBF subnets. It was first trained using the dataset from normal state without fault, and then a residual error generator was designed to detect failures based on the trained CPRBF network. Then, failure detection can be achieved by the analysis of the residual error. Finally, two case studies are introduced to compare the proposed CPRBF network with traditional RBF networks, in terms of prediction and detection accuracy.

Keywords: Fault detection, Chaotic parallel radial basis function (CPRBF), Hydraulic pump, Residual error generator, Time series prediction

Introduction

Fault detection is becoming important because of the complexity of modern industrial systems and growing demands on quality, cost efficiency, reliability, and safety. Early fault detection is an essential prerequisite for further development of automatic supervision. The interest on fault detection techniques would be increasing correspondingly.

Hydraulic pump is the power source of a hydraulic system in aircraft. Its performance has a direct impact on the stability of the hydraulic system and even on the entire system. It has been proved based on statistical data that hydraulic pump has a higher fault probability over other mechanical systems, thus, it is specifically necessary to investigate and conduct fault detection techniques for hydraulic pump. In this article, considering the complexity of hydraulic system and its severe working conditions, the data-driven fault detection method is suggested and applies to its online fault detection.

Generally, data-driven based fault detection consists of the following aspects: data measurement, data processing, data comparison, and data assessment [1]. Usually, the vibration signal of hydraulic pump is used for fault detection in practice, and artificial neural network (ANN) models have also been widely applied to intelligent fault diagnosis owing to their intrinsic parallel, adaptability, and robustness [2,3].

Current data-driven based fault detection methods for hydraulic pump pay more attentions to not only linear characteristics but also nonlinear ones. In addition, owing to the universal presence of chaotic phenomena and the intrinsic characteristics and complex operation conditions of hydraulic system, strong nonlinearity and chaotic features can be clearly found from the vibration signals of hydraulic pump. Therefore, the research works on chaos-based fault detection for hydraulic pump should have a high engineering application value. Currently, chaotic correlation dimension has been applied well for condition monitoring and fault diagnosis of hydraulic pump. In addition, some research works based on Duffing oscillator and Lyapunov exponent have been employed to qualitatively or quantitatively solve the incipient fault recognition for hydraulic pump, with good diagnosis performance. However, the method

* Correspondence: luchen@buaa.edu.cn
[1]State Key Laboratory of Virtual Reality Technology and systems, Beijing, 100191, People's Republic of China
Full list of author information is available at the end of the article

based on neural network in conjunction with chaos theory has rarely appeared, especially for the fault detection of hydraulic pump [4-7].

Among several types of neural networks, radial basis function (RBF) network has relatively high convergence speed, and can approximate to any nonlinear functions. It has been proved that RBF network has a very high performance, in terms of nonlinear time series prediction, fault diagnosis in industrial systems, sensor and flight control systems, etc. [8-14].

A CPRBF network for fault detection of hydraulic pump is presented in this article. This CPRBF network was first trained using the dataset from the normal state without fault of hydraulic pump, and then a residual error generator was designed to detect several types of failures of hydraulic pump based on the trained CPRBF network with one-step prediction of chaotic time series. The proposed model, based on Camastra and Colla's approach [15] and Yang et al.' method [16], is able to reduce the effect of cumulative error and improve the prediction accuracy of RBF.

This article is divided into three sections as follows: Section "Phase-space reconstruction of chaotic time series" describes the chaotic theory on phase space reconstruction employed to obtain the estimation of correlation dimension. Section "Model of chaotic time series prediction and fault detection" proposes a new CPRBF network for chaotic time series prediction, and a residual error generator based on CPRBF network was also designed to detect fault. Then, Section "Case studies" gives several case studies, including simulation results of one-step iterative prediction and experimental results of fault detection for hydraulic pump.

Phase-space reconstruction of chaotic time series

An important issue in the study of dynamic systems is the dynamic phase-space reconstruction theory discovered by Packard et al. in 1980 [17]. It regards a one-dimensional chaotic time series as the compressed information of high-dimensional space. The time series $x(t)$, $t = 1,2,3,...,N$ can be represented as a series of points $X(t)$ in a m-dimensional space

$$\mathrm{X}(t) = (x(t), x(t-1), \cdots, x(t-(m-1))) \tag{1}$$

where m is called as the system embedding dimension. In particular, Takens' embedding theory [18] states that, to obtain a dependable phase-space reconstruction of dynamics system, it must be

$$m \geq 2D + 1 \tag{2}$$

where D is the dimension of system attractor. In order to obtain a correct system embedding dimension, starting from the time series, it is necessary to estimate the attractor dimension D.

Among the different dimension definitions, correlation dimension discovered by Grassberger and Procaccia in 1983 [19], is the most popular one due to its calculation simplicity. It is defined as the following. If the correlation integral $C_m(r)$ is defined as

$$C_m(r) = \frac{2}{N(N-1)} \sum_{i=1}^{N} \sum_{j=i+1}^{N} H\left(r - \left|X_i - X_j\right|\right) \tag{3}$$

where H is the Heaviside function, m is the embedding dimension, and N is the number of vectors in reconstructed phase space. It is proved that if r is sufficiently small, and N would be sufficiently large, the correlation dimension D is equal to

$$D = \lim_{r \to 0} \frac{\ln(C_m(r))}{\ln(r)} \tag{4}$$

The algorithm plots a cluster of $\ln C_m(r)$-$\ln(r)$ curves through increasing m until the slope of the curve's linear part is almost constant. Then, the correlation dimension estimation D can be attained using least square regression.

Model of chaotic time series prediction and fault detection

In practice, it is difficult to get the exact estimation value of the minimum embedding dimension through G-P algorithm. Furthermore, a single RBF network uses the estimation value of minimum embedding dimension as the number of its input, usually resulting in an inaccurate output due to the inaccurate estimation of embedding dimension from human factor. Therefore, a PRBF network consisting of multiple RBF subnets is proposed to increase the system performance with decreased error.

Structure of CPRBF

The CPRBF is constituted of multiple RBF networks connected in parallel for time series prediction. The structure of a CPRBF is shown in Figure 1.

The CPRBF consists of n RBF subnets, which are denoted as sub-RBF$_i$ ($i = 1,2,...,n$), respectively. Each sub-RBF subnet realizes one-step prediction independently at $t + 1$. After the training of sub-RBF by historical dataset, one-step predicted value $\hat{x}_i(t+1)$ can be obtained. The final predicted value $\hat{x}(t+1)$ of PRBF can be achieved through proper weighted combination of $\hat{x}_i(t+1)$.

Input nodes of subnet

Estimation value of the minimum embedding dimension is regarded as the number of input nodes in the central

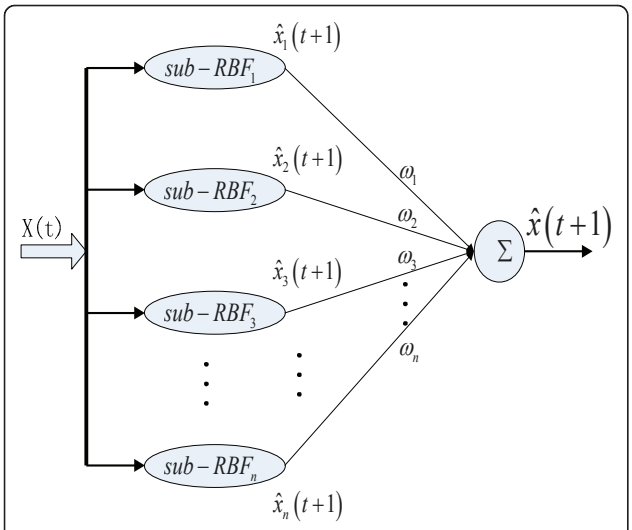

Figure 1 Structure of CPRBF.

subnet, and each of other subnets uses different numbers (calculated based on m) as its input size.

Once the correlation dimension D is obtained by G-P algorithm and least square regression, the number of input nodes in the center subnet sub-$RBF_{[n/2]}$ can be determined as

$$In_{[n/2]} = [2D + 1] \tag{5}$$

where $[\cdot]$ denote an operator of rounded-up, and n is the total number of subnets in PRBF. In_i is the number of input nodes of subnet RBF_i. When $i = [n/2]$, the sub-RBF_i subnet is called the central subnet. Then, the number of input nodes of each subnet can be defined as

$$In_i = In_{[n/2]} + (i - [n/2]) \tag{6}$$

In this article, each subnet RBF_i uses the default parameters: the number of hidden layer is one, and the number of hidden nodes is equal to the number of input vectors.

Calculation of weighted factors

It is necessary to employ weighted factor ω to gain reasonable prediction result because each RBF subnet has different influence on the prediction process. In this article, the optimal weighted value of each subnet is determined according to the minimum predicted absolute percent error (APE) of $\hat{x}_i(t+1)$ in each case. The output of PRBF net is the weighted sum of each individual RBF subnet, and the final predicted result can be represented by the following equation.

$$\hat{x}(t+1) = \sum_{i=1}^{n} \varpi_i \times \hat{x}_i(t+1) \tag{7}$$

where $\hat{x}_i(t+1)$ is the output of ith subnet, and $\hat{x}(t+1)$ is the output of CPRBF network. Then, the least square algorithm is employed to calculate the optimal weighted factors.

$$\min J_{CPRBF} = \min \sum_{t=1}^{N} [\hat{x}(t+1) - \sum_{i=1}^{n} \omega_i \hat{x}_i(t+1)]^2 \tag{8}$$

where N is the number of samples.

Residual error generator

Residual error generator can be designed for fault detection optimization based on CPRBF network and CPRBF prediction process, and it provides a basis for the analysis and calculation of the model uncertainty robustness. The structure of a residual error generator is shown in Figure 2, where $x(t)$ is the time series which can be observed of actual system, CPRBF is the residual error generator model trained using the dataset under normal state, $\hat{x}(t)$ is the one-step prediction value of system, and $e(t)$ is the output of residual error generator.

Evaluation of residual error

Residual error evaluation is an important step of fault detection. In this article, threshold selector is adopted to evaluate the residual error. The concept of threshold selector is firstly introduced systematically in [20] to

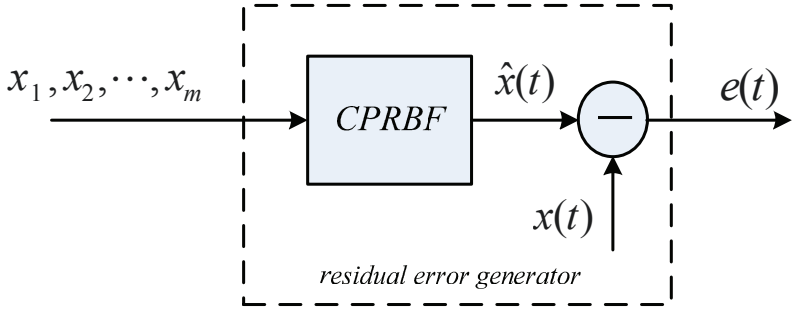

Figure 2 Structure of residual error generator based on CPRBF network.

solve the residual error evaluation problem of LTI systems with model uncertainty. The diagnostic decision is obtained based on the following rule:

$r_{\text{eval}} > J_{th} \rightarrow$ fault state detected

$r_{\text{eval}} \leq J_{th} \rightarrow$ normal state

where r_{eval} is a function related to residual error signal and employed to measure its deviation value, J_{th} is the threshold.

The variance of residual error signal can be adopted as residual error evaluation function.

$$r_{\text{eval}} = \frac{1}{n-1} \sum_{i=1}^{n} (e_i(t) - E(e(t)))^2 \tag{9}$$

The corresponding standard of threshold value can also be determined based on diagnostic experiences in conjunction with different working conditions.

Process of fault detection

Process of fault diagnosis based on CPRBF and residual error generator is shown in Figure 3.

The detailed process is described as below:

- Step 1. Normalize the original time series from diagnosed system
- Step 2. Determine the number of input nodes of each subnet in CPRBF according to G-P algorithm and Takens' theory

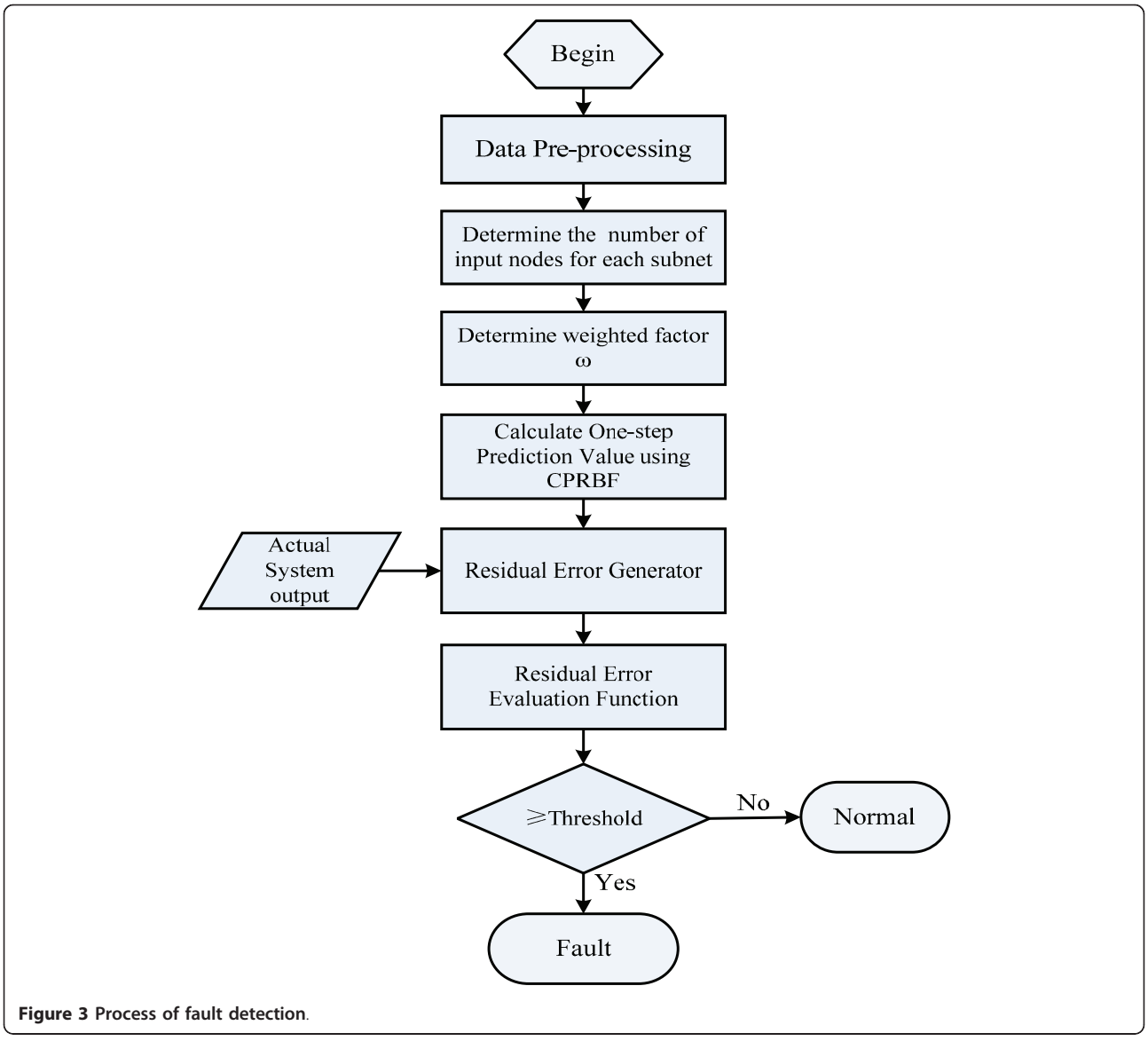

Figure 3 Process of fault detection.

• Step 3. Determine weighted factor ω based on the one-step prediction result of each subnet
• Step 4. Calculate the final one-step prediction output of CPRBF
• Step 5. Construct a residual error generator, and calculate the residual error according to the predicted output and the corresponding system output
• Step 6. Choose a residual error evaluation function with a threshold standard
• Step 7. Fault can be detected based on the evaluation function, with a fault alarm, once the residual error exceeds the threshold value.

Case studies

Verification results of one-step iterative prediction

Considering the lack of practicability from a common one-step prediction method, one-step iterative prediction should be adopted to verify the prediction performance instead. In general, each predicted result at Step 4 is consecutively used as the next input data to achieve one-step iterative prediction. The future trend of actual case (Lorenz's attractor, hydraulic pump) can be obtained gradually with the repetition of Steps 3 and 4, and the loop times depends on the length of actual expected data.

Simulation of Lorenz's attractor

In this section, the simulation result of Lorenz's attractor data is given to verify the performance of the proposed method. Equation 10 is employed to generate the Lorenz's time series data.

$$\begin{cases} dx = -\sigma x + \sigma y \\ dy = -xz + rz - y \\ dz = xy - bz \end{cases} \tag{10}$$

where σ = 16, r = 45.95, b = 4. 1,000 points of X-component Lorenz time series data were first normalized and used for the following prediction.

According to G-P algorithm, a cluster of ln$C_m(r)$-ln(r) curves is plotted with the increase of the embedding dimension m. The correlation dimension can be determined correspondingly, D = 1.7643. According to Equation 2, m = 5 (Figure 4).

As a whole, 1,000 points were divided into two groups (training and testing dataset). The first 800 samples were used for RBF network training. The next 100 samples were used to determine the optimal weighted factor ω, and the last 100 samples for testing of the prediction accuracy between RBF and CPRBF. The number of input nodes of central subnet in the PRBF was 5, obtained from the estimation of the minimum embedding dimension. After the training of each subnet, the optimal weighted factor ω can be obtained via least square algorithm. The parameters of CPRBF are listed as below.

$$\mathrm{In}_{\lfloor n/2 \rfloor} = 5; \quad \mathrm{In}_{\mathrm{in}} = [3, 4, 5, 6, 7]; \quad \varpi = [0.0181\ 0.0196\ 0.8829\ 0.0749\ 0.000]$$

Figure 5 shows the one-step iterative predicted result on the last 100 points of Lorenz's time series by CPRBF network. Figure 6 shows the comparison on APE of Lorenz time series between RBF and CPRBF.

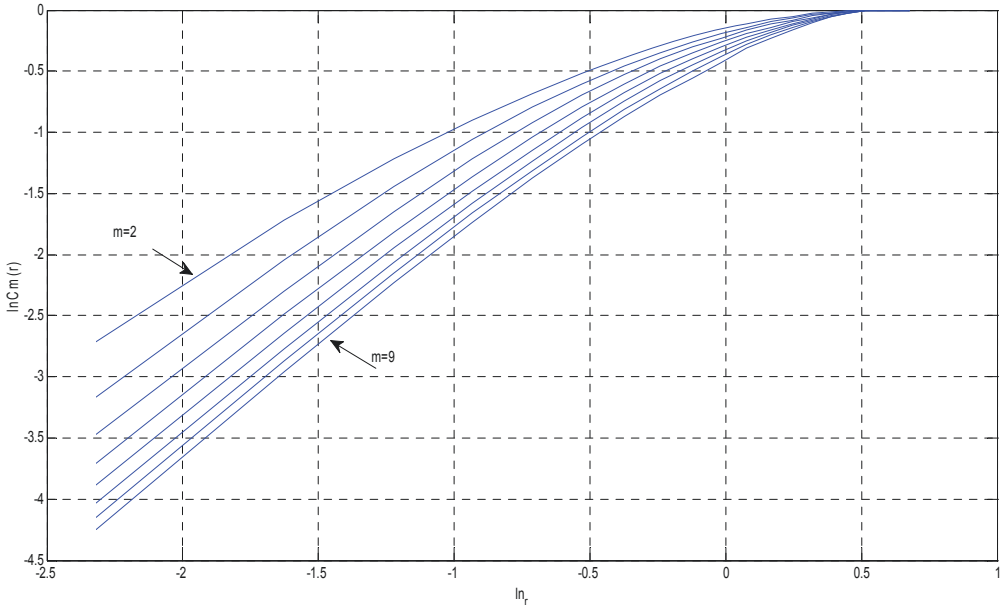

Figure 4 Plot of ln$C_m(r)$-ln(r) of Lorenz time series.

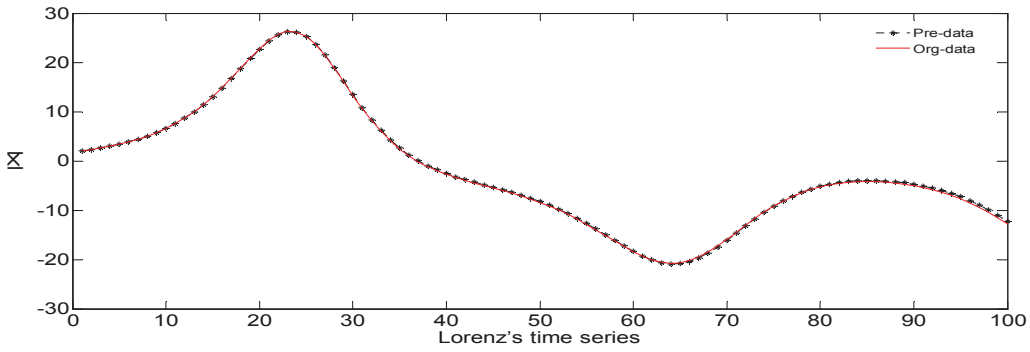

Figure 5 One-step iterative predicted result of Lorenz time series.

Figures 5 and 6 prove that:

- One-step iterative prediction based on CPRBF network has good prediction performance
- Comparing with RBF network, CPRBF network has better performance on iterative prediction, in terms of convergence and stability.

Experimental result using real data of hydraulic pump

In this section, several groups of time series data (normal and fault conditions) were generated from a test rig of SCY Hydraulic pump. Table 1 shows the corresponding maximum Lyapunov exponents ($\lambda_{\max}$) of the above time series. Because all $\lambda_{\max}$ values are positive, the experimental data can be regarded as chaotic time series.

According to G-P method, a cluster of $\ln C_m(r)$-$\ln(r)$ curves for Data 1 is plotted with the increase of the embedding dimension m as shown in Figure 7. The correlation dimension can be determined correspondingly, D = 2.2346. According to Equation 2, m = 6 (Figure 7).

In this case, 800 points of time series data from the vibration signal of hydraulic pump were used for prediction. As a whole, 800 data points were divided into training and testing dataset. The first 600 samples were employed for RBF network training, the next 100 samples for the determination of the optimal weighted factor ω, and the last 100 samples for testing of prediction accuracy between RBF and PRBF. The number of input nodes (minimum embedding dimension) is 5 according to the aforementioned approach. After the training of each subnet, the weighted factor ω can also be obtained. The parameters of CPRBF are

$$\mathrm{In}_{[n/2]} = 6; \quad \mathrm{In}_{\mathrm{in}} = [4, 5, 6, 7, 8]; \quad \varpi = [0.0000\ 0.1610\ 0.2221\ 0.2886\ 0.3283]$$

Figure 8 shows the result using one-step iterative prediction based CPRBF network. Figure 9 presents the comparison of APE error between RBF and CPRBF, and both are all based on Data 1.

Comparing with RBF network, PRBF model has higher prediction accuracy, without the effect of error accumulation.

Experimental results of fault detection for hydraulic pump

Construction of detection model using CPRBF

According to the G-P method, a cluster of $\ln C_m(r)$-$\ln(r)$ curves of normal data is plotted with the increase of the

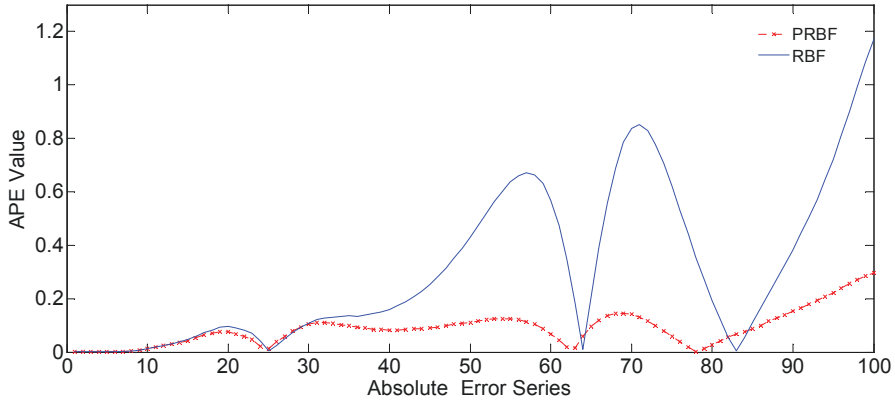

Figure 6 Comparison of APE between RBF and CPRBF.

Table 1 Lyapunovs of hydraulic pump's sample data

Data	λ_{max}
Data1	0.0508
Data2	0.0744
Data3	0.0435

embedding dimension m, as shown in Figure 10. The correlation dimension can be determined correspondingly, D = 2.2472. According to Equation 2, m = 6.

In this case, 800 points of time series data from the vibration signal without fault were used for the construction of detection model. As a whole, 800 data points were divided into training and testing dataset. The first 600 samples were employed for network training, the next 100 samples for the determination of the optimal weighted factor ω, and the last 100 samples for determination of the threshold of fault detection. After training and testing, prediction model of normal state can be determined. The parameters of CPRBF are shown as below.

$$\mathrm{In}_{[n/2]} = 6; \quad \mathrm{In}_{in} = [4, 5, 6, 7, 8]; \quad \varpi = [0.0462\ 0.0000\ 0.3696\ 0.3558\ 0.2283]$$

Figure 11 shows the residual error of normal data, and CPRBF based model has better prediction performance with an accuracy of about 10^{-6}.

Residual error signals of hydraulic pump based on CPRBF network

Wear fault of valve plate Dry friction is probably caused by fatigue crack, surface wear, or cavitation erosion, etc. In case of this failure, with the increasing of moment coefficient between rotor and valve plate, contact stress grows and oil film becomes thinner. Further, as a repetitive impact of the contact stress, the surface of valve plate is fatigued and spalls. As a result, dry friction appears, with an increment of motion gap of hydraulic pump and a decrement of volumetric efficiency. Meanwhile, the dry friction inevitably generates additional vibration signals in the valve plate's shell near the high pressure chamber.

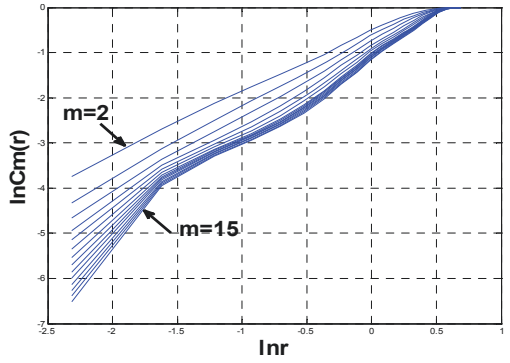

Figure 7 Plot of $\ln C_m(r)$-$\ln(r)$ of hydraulic pump's sample data.

In this article, 100 points of time series data from the vibration signal with valve plate rotor wear were used for detection according to the aforementioned method. Figure 12 shows the residual error of valve plate rotor wear.

Wear fault between swash plate and slipper Dry friction, caused by oil impurities or small holes on plunger ball, etc., usually results in wear or burnout of the faying surface between swash plate and slipper, which probably causes the falling of slipper, and affects the performance of hydraulic pump.

Similar to the above case study, 100 points of time series data from the vibration signal with wear fault between swash plate and slipper of hydraulic pump were used for fault detection. Figure 13 shows the residual error of wear fault between swash plate and slipper.

Fault detection

Threshold value is a key point in fault decision-making, due to uncertainties in practical and external disturbances. The rate of fail-to-report increases if the threshold is too large, vice versa, the rate of false alarm would increase. Appropriate threshold should be selected according to the analysis, with the support of residual error evaluation function proposed, on hydraulic pump's normal and faulty data.

Two groups of normal data and six groups of faulty data from a testing hydraulic pump were used for analysis. Residual error series were obtained, respectively, via residual error generator designed using CPRBF network, and each variance of residual error series was calculated correspondingly. Table 2 shows the variance values.

It can be seen obviously from Table 2 that, two magnitude levels of residual error's variance values between normal and fault states are clearly distinct. According to experience, the threshold can be determined with a standard of 10 times higher than the mean of variances under normal states. Here, J_{th} = 3.196e-005. It should be also noticed that, the threshold standard must be readjusted according to different working conditions.

The variance values of the above two cases are 3.7781e-004 and 1.7305e-004, respectively. These values are greater than J_{th}, thus, the fault can be detected based on the variance of residual error signal.

Conclusions

It is shown from the simulation results that, CPRBF network model, in conjunction with phase space reconstruction, show better capabilities and reliability in predicting chaotic time series, as well as a high performance of convergence ability and prediction precision on short-term prediction of chaotic time series.

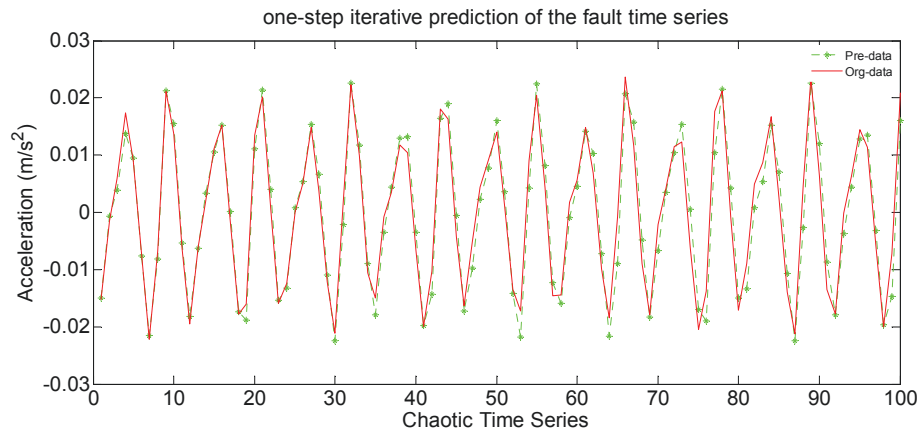

Figure 8 One-step iterative predicted result of Data1.

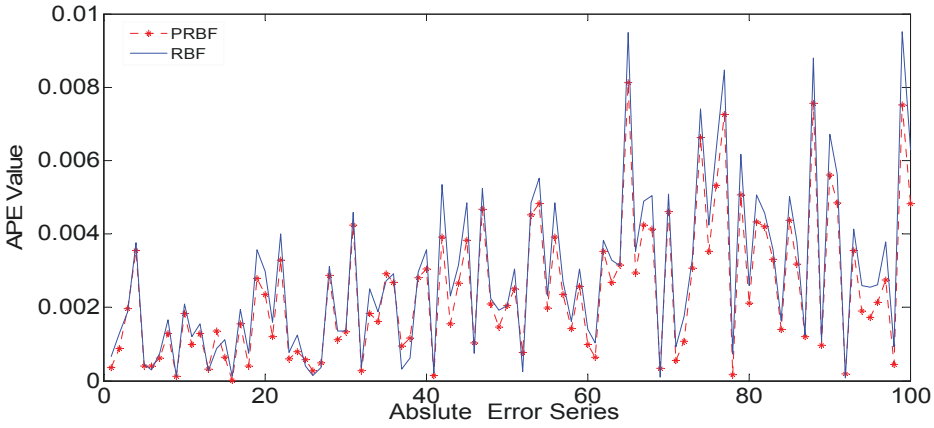

Figure 9 Comparison of APE between RBF and CPRBF.

The experimental results show that, CPRBF model has high ability in approximation to the output and state of a normal system, which is useful for fault detection. The CPRBF network can memorize various nonlinear states or interferences of a system with normal states, therefore, the actual system output will be different with the predicted output of CPRBF network once any anomaly occurs, and the system can be regarded as faulty state if the residual error exceeds the threshold. Thus, CPRBF network based method is effective to real-time

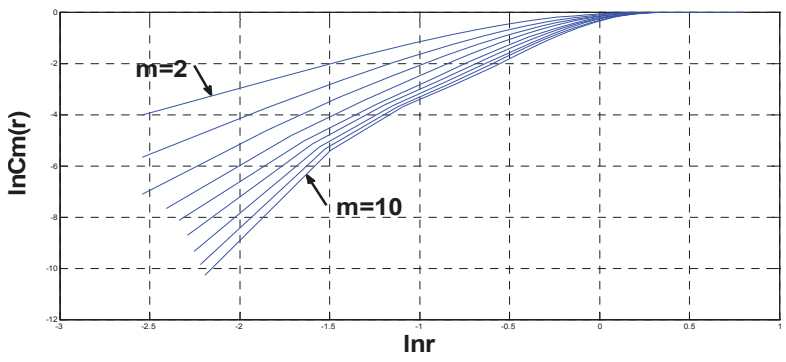

Figure 10 Plot of $\ln C_m(r)$-$\ln(r)$ of hydraulic pump's data.

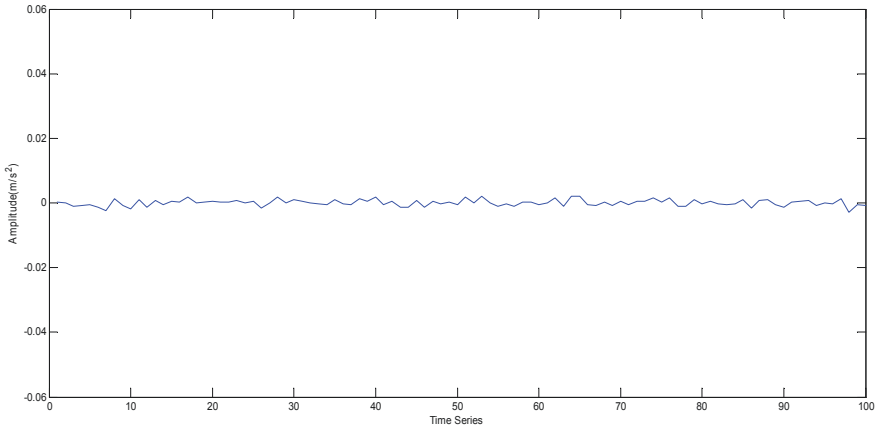

Figure 11 Residual error of normal data.

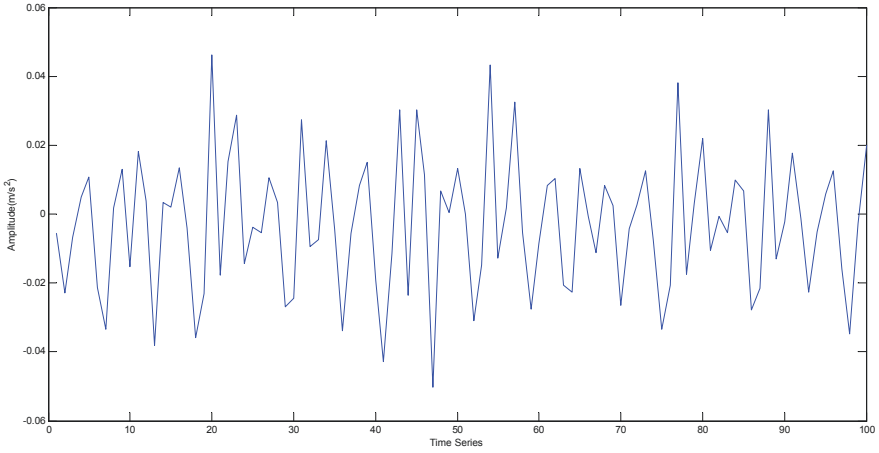

Figure 12 Residual error of valve plate rotor wear.

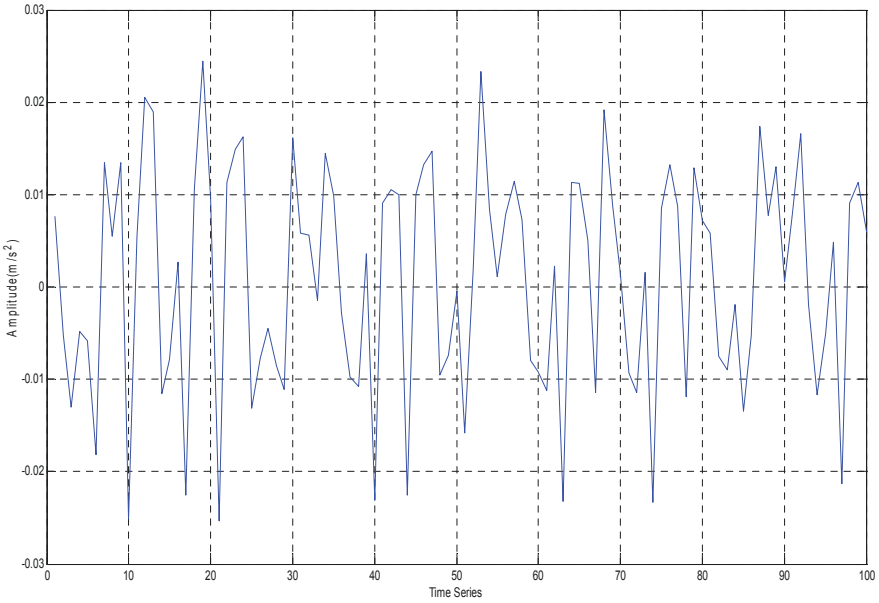

Figure 13 Residual error of wear fault between swash plate and slipper.

Table 2 Variance values of residual error series

State	Residual error signal							
	Normal (e-006)		Fault (e-004)					
Data	Normal 1	Normal 2	Fault 1	Fault 2	Fault 3	Fault 4	Fault 5	Fault 6
Variance	3.0529	4.7796	1.3400	1.2244	1.0634	1.0831	2.6596	2.5383
Mean of variance	3.91625		1.651467					

fault detection. However, it is also shown from the experiments that different types of faults might represent the same fault form, accordingly, the proposed method is not suitable for performing fault location but for conducting condition monitoring. Further work will focus on how to isolate any type of fault and identify its fault classification.

This article mainly aims to discuss the feasibility and possibility of practical fault detection for hydraulic pump using neural network in conjunction with chaos theory. A commonly used neural network in the past and now, namely, RBF network was employed for fault detection for hydraulic pump in conjunction with chaos theory. Certainly, methods using chaos theory combined with other popular ANNs should be also our emphasis in the following works. As known, support vector machine (SVM) has been widely applied in many fields. Compared with other ANNs, SVM overcomes many defects, such as over-fitting, local convergence. In addition, SVM has advantages over other ANNs, in terms of robustness and prevention of curse of dimensionality, etc. Thus, our further work will focus on SVM in conjunction with chaos theory, especially for those modified SVM.

Acknowledgements
The research is supported by the National Natural Science Foundation of China (Grant Nos. 61074083, 50705005), as well as the Technology Foundation Program of National Defense (Grant No. Z132010B004). The authors are also very grateful to the reviewers and the editor for their valuable suggestions.

Author details
[1]State Key Laboratory of Virtual Reality Technology and systems, Beijing, 100191, People's Republic of China [2]School of Reliability and Systems Engineering, Beihang University, Beijing, 100191, People's Republic of China [3]Department of Foundation Science, The First Aeronautical Institute of Air Force, Xinyang 464000, People's Republic of China

Competing interests
The authors declare that they have no competing interests.

Received: 27 December 2010 Accepted: 30 August 2011
Published: 30 August 2011

References
1. KY Chen, CP Lim, WK Lai, Application of a neural fuzzy system with rule extraction to fault detection and diagnosis. J Intell Manuf. **16**, 679–691 (2005). doi:10.1007/s10845-005-4371-1
2. MM Hanna, A Buck, R Smith, Fuzzy petri nets with neural networks to model products quality from a CNC-milling machining centre. IEEE Trans Syst Man Cyber A **26**, 638–645 (1996). doi:10.1109/3468.531910
3. MM Polycarpou, AJ Helmicki, Automated fault detection and accommodation: a learning system approach. IEEE Trans Syst Man Cyber. **25**, 1447–1458 (1995). doi:10.1109/21.467710
4. WL Jiang, DN Chen, CY Yao, Correlation dimension analytical method and its application in fault diagnosis of hydraulic pump. Chin J Sens Actuators **17**(1), 62–65 (2004)
5. WL Jiang, YM Zhang, HJ Wang, Hydraulic pump fault diagnosis method based on lyapunov exponent analysis. Mach Tool Hydraulics **36**(3), 183–184 (2008)
6. QJ Wang, XB Zhang, HP Zhang, Y Sun, Application of fractal theory of fault diagnosis for hydraulic pump. J Dalian Maritime Univ. **30**(2), 40–43 (2004)
7. YL Cai, HM Liu, C Lu, JH Luan, WK Hou, Incipient fault detection for plunger ball of hydraulic pump based on Duffing oscillator. Aerosp Mater Technol. **39**(suppl), 302–305 (2009)
8. J Park, IW Sandberg, Universal approximation using radial-basis-function networks. Neural Comput. **3**(2), 246–257 (1991). doi:10.1162/neco.1991.3.2.246
9. T Poggio, F Girosi, Networks for approximation and learning. Proc IEEE. **78**(9), 1481–1497 (1990). doi:10.1109/5.58326
10. S Chen, Nonlinear time series modeling and prediction using Gaussian RBF networks with enhanced clustering and RLS learning. Electron Lett. **31**(2), 117–118 (1995). doi:10.1049/el:19950085
11. MAS Potts, DS Broomhead, Time series prediction with a radial basis function neural network. SPIE Adapt Signal Process. **1565**, 255–266 (1991)
12. KG Narendra, VK Sood, K Khorasani, R Patel, Application of a radial basis function (RBF) neural network for fault diagnosis in a HVDC system. IEEE Trans Power Syst. **13**(1), 177–183 (1998). doi:10.1109/59.651633
13. DL Yu, JB Gomm, D Williams, Sensor fault diagnosis in a chemical process via RBF neural networks. Control Eng Practice **7**(1), 49–55 (1999). doi:10.1016/S0967-0661(98)00167-1
14. YM Chen, ML Lee, Neural networks-based scheme for system failure detection and diagnosis. Math Comput Simul. **58**(2), 101–109 (2002). doi:10.1016/S0378-4754(01)00330-5
15. F Camastra, AM Colla, Neural short-term prediction based on dynamics reconstruction. Neural Process Lett. **9**, 45–52 (1999). doi:10.1023/A:1018619928149
16. HY Yang, H Ye, GZ Wang, MY Zhong, A PMLP based method for chaotic time series prediction, in *Proceedings of the 16th IFAC World Congress, Mo-E11-To/2* (2005)
17. N Packard, J Crutcheld, J Farmer, R Shaw, Geometry from a time series. Phys Rev Lett. **45**, 712–716 (1980). doi:10.1103/PhysRevLett.45.712
18. F Takens, Detecting strange attractors in turbulence. Dynamical Systems and Turbulence, Warwick 1980, Lecture Notes in Mathematics 898 (Springer, Berlin) 366–381 (1981)
19. P Grassberger, I Procaccia, Measuring the strangeness of strange attractors. Physica **D9**, 189–208 (1983)
20. A Emami-Naeini, MM Akhter, SM Rock, Effect of model uncertainty on failure detection: the threshold selector. IEEE Trans Autom Control **33**, 1106–1115 (1988). doi:10.1109/9.14432

doi:10.1186/1687-6180-2011-49
Cite this article as: Lu *et al.*: **Fault detection for hydraulic pump based on chaotic parallel RBF network.** *EURASIP Journal on Advances in Signal Processing* 2011 **2011**:49.